Acinar Tight Junctions are Altered in an Early Phase of Acute Edematous Pancreatitis in a Rat Pancreatic Duct Ligation Model

Ogata S[1,2], Tsuwano S[3,4], Tamai S[2,5] and Nakanishi K[1,2*]

[1]Department of Pathology and Laboratory Medicine, National Defense Medical College, Tokorozawa, Japan

[2]Department of Laboratory Medicine, National Defense Medical College Hospital, Tokorozawa, Japan

[3]Department of Surgery, National Defense Medical College, Tokorozawa, Japan

[4]Department of Surgery, Saitama National Hospital, Wako, Japan

[5]Department of Pathology, Tokyo Saiseikai Central Hospital, Minato, Japan

Abstract

Background: Although trypsin autoactivation in acinar cells is considered to be an initial event in acute human pancreatitis, mild pancreatitis with/without trypsin autoactivation is common in human acute pancreatitis, and interstitial edema is one of its characteristic features. **Methods:** To elucidate the mechanism underlying such interstitial edema in acute edematous pancreatitis, we examined the condition of intercellular junction complexes between acinar cells in the initial phase of pancreatitis in a rat pancreatic duct ligation model. For this experiment, serum and pancreatic tissues were obtained at 30, 60, 120, and 180 mins after duct ligation and compared biochemically, morphologically, and immunofluorescently with samples from control or sham-operated rats. **Results:** In the present experiments, both the tissue water content and the serum amylase values were elevated only in the group 180 min after duct ligation. Tissue trypsin values revealed no significant changes, and histology did not reveal tissue necrosis. In an immunofluorescence study, acinar luminal staining for the tight junction-protein ZO-1 was significantly less distinct in both the groups 120 min and 180 min after duct ligation, although the adherens junction proteins pan-cadherin and β-catenin showed no significant changes throughout the course of the experiment. Ultrastructurally, tight junctions in both groups (120 and 180 mins) appeared leaky (not closed) more frequently than in other groups. **Conclusions:** Acinar tight junctions were altered in an early phase of pancreatitis in the present acute edematous pancreatitis model, and such alterations may contribute to the interstitial edema formation that is characteristic of mild pancreatitis.

Key words: Acute pancreatitis; Duct hypertension; Edema; Tight junction

Abbreviations

IF: Immunofluorescent; CBPD: Common Biliopancreatic Duct; JC: Junctional Complex; PDL: Pancreatic Duct Ligation; DAPI: 4,6-Diamidino-2-Phenylindole Dihydrochloride Hydrate; ER: Endoplasmic Reticulum; TJ: Tight Junction; AJ: Adherens Junction.

Introduction

Acute pancreatitis is an inflammatory disease involving complex systemic changes, and trypsin autoactivation has been described as the initial mechanism in an opossum model of common biliopancreatic duct (CBPD) obstruction [1]. However, disturbances of the microcirculation regulated by sensory nerves play an important role in the initiation and progression of acute pancreatitis. The activation of sensory nerves containing a variety of receptors and ion channels, such as nociceptive ion-channel transient receptor potential vanilloid type 1 (TRPV1), causes the release of inflammatory neuropeptides, such as substance P and calcitonin gene-related peptide (CGRP), leading to local vasodilation and plasma extravasation. The local angiotensin-renin system was also reported to be involved in nuclear transcription factor NF-κB activation [2]. Furthermore, proinflammatory mediators, such as capsaicin (a neural product of the hot pepper plant) and

leukotriene B4 (a lipid mediator), regulate TRPV1 directly or indirectly on sensory nerves [3], whereas CGRP reduces NF-κB-related inflammatory gene products of proinflammatory cytokines and adhesion protein molecules [4]. Recently, the immunohistochemical expression of TRPV1, insulin receptor, substance P, and CGRP was reported to colocalize at the pancreas dorsal root ganglion and nodose ganglion neurons, suggesting a role for their functional interaction [5,6].

In routine practice, most human acute pancreatitis is mild and self-limiting [7]. Trypsin autoactivation and NF-κB activation may be limited in mild pancreatitis without tissue necrosis. Morphologically, interstitial edema is commonly observed in acute pancreatitis with or without tissue necrosis. The mechanism leading to the formation of interstitial edema is now considered to involve an increase in vascular permeability secondary to cytokine release from the injured tissue, periacinar myofibroblasts, and leukocytes [8-10]. This idea seems to fit the formation of interstitial edema in severe pancreatitis with tissue necrosis, in which leakage of cellular contents from degenerated acinar cells or misplaced exocytosis due to a derangement in cell polarity develops. Concerning mild pancreatitis without tissue necrosis, we asked the simple question of whether or not interstitial edema formation might be triggered by increased vascular permeability. Indeed, some researchers have reported changes in duct and acinar permeability, suggesting increases in

paracellular permeability, in various pancreatitis models [11-15].

To examine paracellular permeability in relation to interstitial edema formation in the initial phase of mild pancreatitis, we focused on specialized plasma membrane structures called junctional complexes (JCs), which are observed at the cell-cell border and are composed of occluding junctions and anchoring junctions [16]. In pancreatic acini, tight junctions (TJs) correspond to occluding junctions and function as seals with fused plasma membranes, thereby blocking the leakage of intra-luminal fluid into the paracellular spaces. If these structures are damaged in acute pancreatitis, the paracellular permeability would be increased, and the leakage of luminal fluid would lead to interstitial edema.

We selected an acute edematous pancreatitis model involving pancreatic duct ligation (PDL) in rats rather than an opossum model of CBPD obstruction. Using this model, we confirmed immunofluorescently and ultrastructurally whether or not TJs showed changes in the initial phase of pancreatitis without tissue necrosis.

Materials and Methods

Animal preparation

Male Sprague-Dawley rats (12-15 weeks, weight 330-480 g; SLC, Inc., Shizuoka, Japan) were kept preoperatively with overnight fasting but with water freely available. Under anesthesia achieved by the intraperitoneal administration of sodium pentobarbiturate (5 mg per 100 g body weight; Dai-Nippon Pharmaceuticals, Co., Ltd., Osaka, Japan), a midline-laparotomy was performed on these rats. In the PDL group rats, pancreata were separated from the loose connective tissues, and careful ligation was performed using a silk suture, avoiding the occlusion of major vasculatures. The ligation site was 1-2 cm away from the spleen, and a substantial amount of pancreata with intact CBPD remained downstream of the ligation site. Rats were killed 30, 60, 120, or 180 min after duct ligation (PDL30′, PDL60′, PDL120′ and PDL180′ groups, respectively), and then pancreata distal to the ligation sites were excised. Cardiac blood samples were also collected.

Control rats received only anesthesia and were then killed. Sham group rats received almost the exact same procedure as the PDL groups but without ligation, and samples were collected at the time points corresponding to those of the PDL groups (sham30′, sham60′, sham120′ and sham180′ groups, respectively). Each group comprised 6-9 rats.

These procedures were performed in accordance with the guiding principles of the National Institute of Health and with the permission of the institutional Animal Care and Use Committee.

Biochemical analyses and tissue water content estimation

Serum samples were collected from centrifuged cardiac blood samples. Serum amylase values were determined with the aid of Infinity Amylase reagent (Sigma Diagnostics, Inc.,

St. Louis, MO, USA) containing 4,6-ethylidene (G1)-p-nitrophenyl(G7)-alpha1-D-maltoheptoside, alpha-glucosidase, sodium chloride, and buffer (pH 7.0). In brief, serum samples were added to the reagent, and the amylase activities were calculated using the manufacturer's protocol based on the increased rate of absorption at 405 nm in a spectrophotometer.

Excised fresh pancreatic tissues were divided for the estimation of the water content and the assay of the trypsin activity. To estimate the water content, pancreatic tissues (wet) were kept in a desiccator until there was no longer any change in the weight, and the tissue water content was calculated from the tissue weights before and after desiccation. For the trypsin assay, pancreatic tissues were manually homogenated in 0.001N hydrochloride solution on ice. After centrifugation at 10,000 rpm for 10 mins at 4°C, the supernatant was added to mixtures of 0.046 M Tris-HCl buffer (pH 8.1; with 0.0115 M calcium chloride) and 0.01 M p-toluene-sulfonyl-L-arginine methyl ester (Sigma Diagnostics, Inc.). The trypsin concentration was calculated according to the manufacturer's instructions from the increased rate of absorption at 247 nm in a spectrophotometer.

Histology

Sampled pancreatic tissues were fixed in 4% paraformaldehyde for routine histology. Paraformaldehyde-fixed materials were dehydrated with methanol, permeated with xylene and then with paraffin, and finally embedded in paraffin wax. From tissue paraffin blocks, sections 4 µm thick were cut onto silane-coated glass slides. After deparaffinization, samples were stained with hematoxylin and eosin. Glass slides were observed under an Olympus BX50 microscope (Olympus Co., Tokyo, Japan), and images were acquired through a Fujix HC-2500 digital camera with the Photograb software program, version 1.0 (Fuji Photo Film, Co., Ltd., Tokyo, Japan). These images were examined for evidence of interstitial edema, "focal acinar cell necrosis" (see Discussion), interstitial neutrophilic infiltration, and tissue necrosis.

Immunofluorescence

Fresh pancreatic tissues were embedded in OTC compound (Sakura Finetechnical, Co., Ltd., Tokyo, Japan) and immersed in liquid nitrogen. From these frozen samples, sections 5 µm thick were cut onto silane-coated glass slides and fixed with acetone at –20°C. By staining with 4,6-diamidino-2-phenylindole dihydrochloride hydrate (DAPI, 300 nM; Molecular Probes, Inc., Eugine, MA, USA) and/or Alexa Fluor 633-labeled Phalloidin (1 unit per slide; Molecular Probes, Inc.), we performed multiple immunofluorescent methods to analyze TJ proteins. We also analyzed the adherens junctions (AJs), which consist of JCs. We used anti-ZO-1 (goat polyclonal, 2 µg/mL; Santa Cruz Biotechnology, Inc., Santa Cruz, CA) and anti-7H6 (mouse clone 7H6, 5 µg/mL; American Research Products, Inc., Belmont, MA) antibodies (to examine TJ-associated proteins) as well as antibodies against pan-cadherin (goat polyclonal, 4 µg/mL; Santa Cruz Biotechnology, Inc.) and β-catenin (mouse

clone E-5, 4 µg/mL; Santa Cruz Biotechnology, Inc.) (AJ-structural and AJ-associated proteins).

After blocking non-specific staining with DAKO serum-free blocking reagent (DAKO Cytomation, Kyoto, Japan), slides were incubated in an overnight cocktail of the two primary antibodies at 4°C. Then, corresponding Alexa Fluor dye-labeled secondary antibodies (Molecular Probes, Inc.) were incubated for one hour each. Finally, slides were incubated at room temperature for 20 min in a mixture of DAPI and/or labeled Phalloidin. Between procedures, glass slides were washed 3 times with TBS-T (0.05 M Tris-HCl, 0.15 M NaCl, pH 7.8, containing 0.1% Triton X). We stained rat liver tissue as positive control slides and incubated some slides with labeled secondary antibodies without the primary antibodies as a negative control. The glass slides were observed by confocal laser microscopy (LSM510) using the LSM510 software program, version 2.5 (Carl Zeiss, Jena, Germany). We acquired 7-9 images from each specimen using a C-apochromat 63x/1.2 W Corr objective lens (Carl Zeiss) and the multi-track line scanning condition (8-bit depth, 512 × 512 pixels, average 8 times [mean method], zoom 1.4). Adequate beam-splitter and band-pass filters were selected for image acquisition.

In the pancreata of control and sham groups treated with TJ protein antibodies, acinar lumens were highlighted, while with AJ-structural and AJ-associated protein antibodies, acinar lumens and basolateral plasma membranes of acinar cells were stained well. Two of our group (S.O and S.T) classified acini as to whether or not the labeled dyes had highlighted luminal and/or basolateral plasma membrane structures distinctly. We counted the numbers of acini with immunofluorescently distinct lumens in the images acquired from each specimen and then calculated the proportion displaying distinct lumens.

Electron microscopy

For electron microscopy, tissues were excised at about 1-mm3 size, pre-fixed with 2.5% glutaraldehyde for 48-72 h, and post-fixed with 1% osmium tetraoxide for 2 h. After sequential dehydration with ethanol and propylene oxide, samples were permeated and embedded in epon resin. Then, ultrathin sections were stained with uranium acetate and lead citrate and observed using an H-7100 transmission electron microscope (acceleration voltage 75 kV; Hitachi, Ltd., Tokyo, Japan).

We observed each section's morphology with regard to acinar nuclear clumping, dilatation of endoplasmic reticulum (ER), vacuolation, loss of microvilli on acinar lumens, and misplaced (basolateral) exocytosis. We also estimated the frequencies of non-closed, leaky junctions in acinar TJs in samples from each group, although TJs were usually closed (i.e. plasma membranes of neighboring cells arranged in parallel without spaces) [17]. TJs with indistinct plasma-membrane structures were excluded from the count.

Statistical analyses

Statistical analyses were performed using the StatView software program, version 5.0 (SAS Institute, Inc., Cary, NC, USA). A one-way analysis of variance for the serum amylase concentration was performed and followed by a Scheffe F test as a post hoc test. The Kruskal-Wallis test for the tissue water content analysis and frequency analyses relating to the immunofluorescence study were performed and followed by the Mann-Whitney U test with Bonferroni correction. Fisher's exact probability test for frequency analyses in electron microscopy was also performed. P values less than 0.05 were considered significant.

Results

Confirmation of the validity of the rat PDL model

In the present biochemical analysis, the serum amylase values were similar among the control, sham groups, and PDL30′, PDL60′, and PDL120′ groups; however, that for the PDL180′ group was significantly increased compared with the control and sham180′ groups (Figure 1A). In the tissue water content analysis, the tissue water content ratio of the PDL180′ group (expressed as a percentage of the content in the control group) was significantly greater than the control and sham180′ group values (Figure 1B). A biochemical analysis of the tissue trypsin activity showed no significant differences among the groups (data not shown).
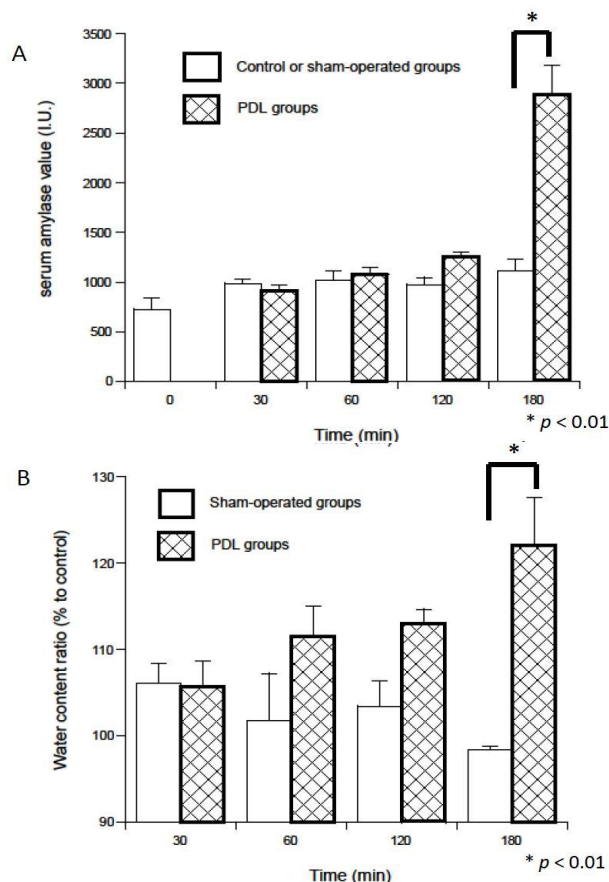

Figure 1A and 1B: Relationships between the time after pancreatic duct ligation and (A) the serum amylase values and

(B) the tissue water content ratio. Compared to the corresponding sham-operated group, samples from the group 180 minutes after duct ligation displayed significant elevations in serum amylase values (A) and the tissue water content ratio (B).

Under light microscopy, the tissue organization was well preserved without significant findings in the control and sham groups. Interstitial edema and "focal acinar cell necrosis" were found rarely in the PDL60′ group, but both were evident in all samples in the PDL120′ and PDL180′ groups, along with mild neutrophilic infiltration (Figure 2AB). No tissue necrosis was observed in any group. Under electron microscopy, a small number of acinar cells exhibited clumping of nuclear chromatin even in the control and sham groups. Some acinar cells displayed mild ER dilatation in the PDL60′ group, and many cells showed ER swelling in the PDL120′ and PDL180′ groups (Figure 2C). In the acinar lumens in some cases in the PDL120′ and PDL180′ groups, loss of microvilli and surface flattening were also seen. Misplaced (i.e. basolateral) exocytosis was not observed in any specimens.
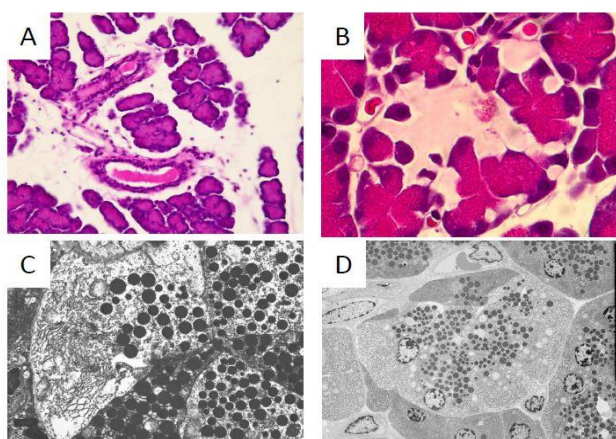

Figure 2: Histological findings on light microscopy (A,B) and electron microscopy (C,D). In the groups 120 and 180 minutes after duct ligation, marked interstitial edema and neutrophilic infiltration (A) and "focal acinar cell necrosis" (B) were observed. Under the same conditions, swelling of the endoplasmic reticulum was observed ultrastructurally in acinar cells (C). Polarization was well preserved in the acinar cells, and zymogen granules were located near the apical lumens (D).

Examination of acinar JCs by immunofluorescence and ultrastructural methods

In our immunofluorescence study for TJ proteins, the staining patterns for anti-ZO-1 and 7H6 antibodies were quite similar in the specimens, but the former was stained more distinctly. In the ZO-1 study, 63% to 70% of acini in the control and sham groups exhibited distinct acinar lumens, although only 26% to 28% of acini in the PDL120′ and PDL180′ groups had immunofluorescently distinct acinar lumens (p<0.01; Figure 3). Regarding AJ proteins, the

staining patterns for anti-pan-cadherin and anti-β-catenin were quite similar among the specimens, although the latter stained more distinctly than the former. We were able to detect distinct immunofluorescence on the luminal and basolateral plasma membranes even in the PDL180′ group (Figure 4), and we noted no significant differences among the groups (data not shown).
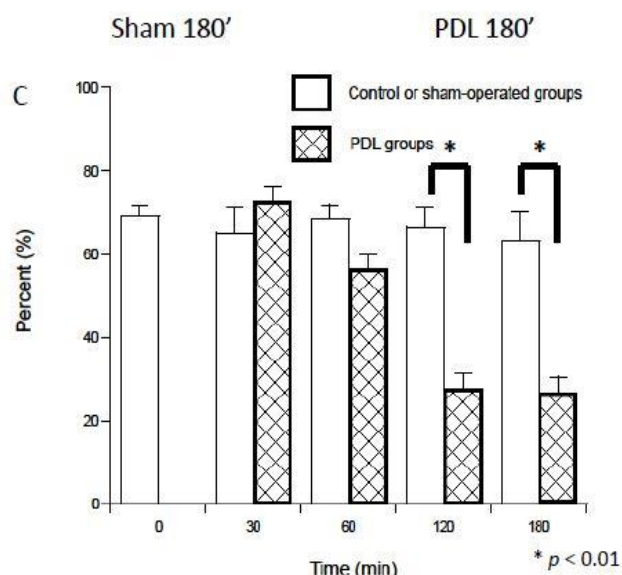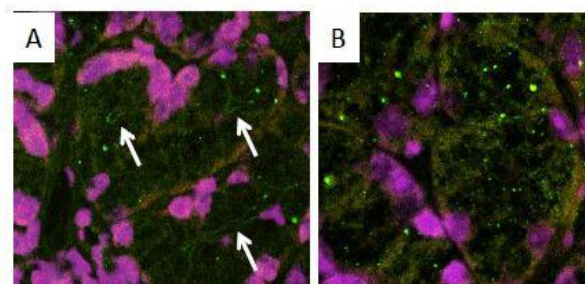

Figure 3: Immunofluorescent images for the tight junction protein ZO-1. Phalloidin (orange) indicates the acinar outline, while DAPI (violet) indicates acinar nuclei. In the center of acini, anti-ZO-1 antibody (green) highlights the acinar lumens (white arrows) in the group 180 minutes after sham-operation (A), but such structures were less evident in the group 180 minutes after pancreatic duct ligation (B). The relationship between the time after pancreatic duct ligation and the percentage of acini displaying distinct lumens in the ZO-1 study (C). This percentage was significantly lower in the groups 120 min and 180 min after duct ligation than in the control and sham groups.

In our electron microscopic search for non-closed, leaky TJs, we counted between 42 and 73 TJs per group in the acini of the control and PDL groups. We found leaky TJs in 21.7% - 28.9% of acinar TJs in the control (13 of 60), PDL30′ (9 of 48), and PDL60′ (18 of 73) groups (Figure 5). However, more than 50% of acinar TJs exhibited leaky morphology in the PDL120′ (22 of 42) and PDL180′ (27 of 53) groups, an

incidence that was significantly greater than in the other

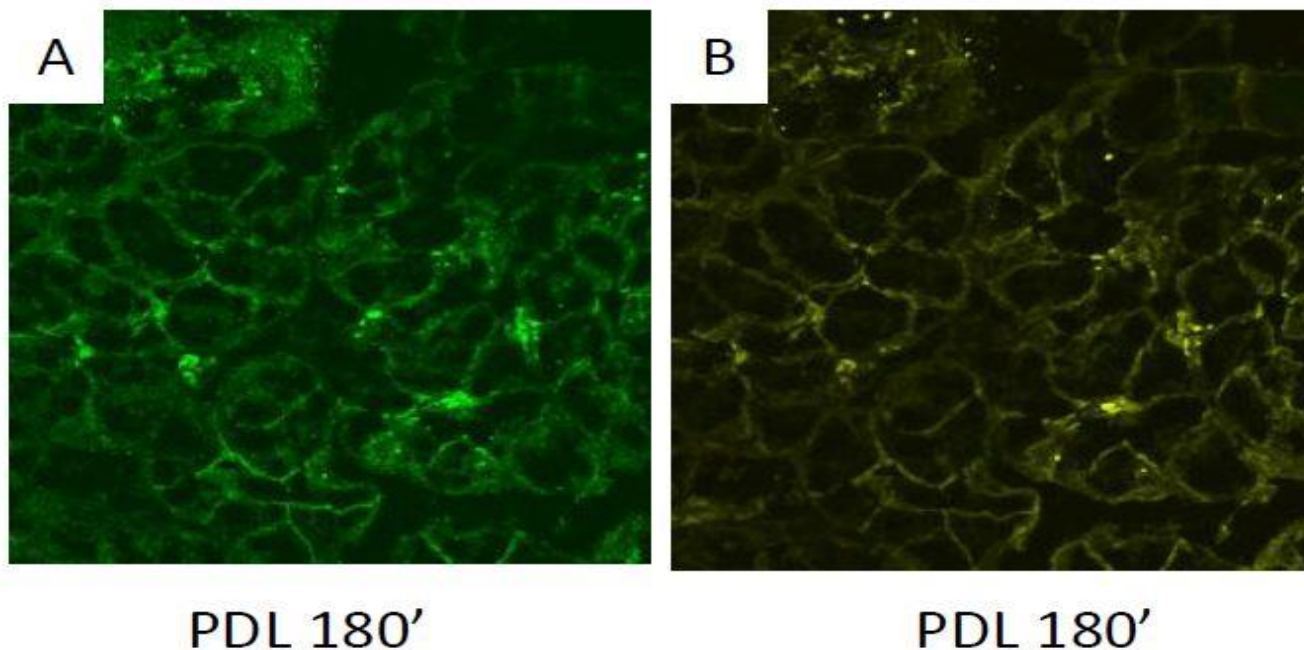groups (control, PDL30′, and PDL60′) ($p < 0.05$).

Figure 4: Immunofluorescent images for the adherens junction proteins pan-cadherin (A) and β-catenin (B). These antibodies highlight the acinar lumens and basolateral membranes of acinar cells even in the group 180 minutes after pancreatic duct ligation.
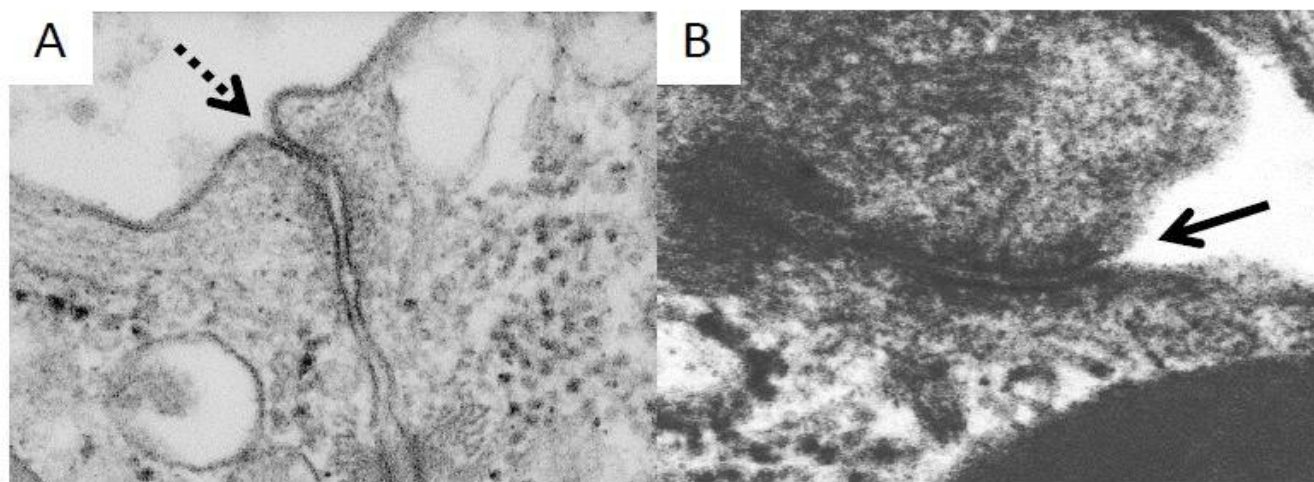

Figure 5: Ultrastructural images of tight junctions between acinar cells. (A) A tight junction (interrupted arrow) that was closed in the group 120 minutes after pancreatic duct ligation. (B) A tight junction that was not closed in the group 180 minutes after pancreatic duct ligation. In the non-closed, leaky tight junction, a space (solid arrow) between two plasma membranes arranged in parallel was observed.

Discussion

In the opossum model of CBPD obstruction, bile reflux into the pancreatic ducts and an elevation in plasma cholecystokinin (CCK) concentration are key characteristic factors [18-23]. To exclude these factors, for the present study we selected the pancreatic duct ligation model. This pancreatic duct ligation was expected to exclude the potential for bile reflux, and duodenal CCK production could be

expected to be suppressed by a substantial volume of pancreata near the duodenum remaining intact (without edema). Thus, the present model might be considered suitable for basic research into human acute pancreatitis, such as biliary or post-endoscopic retrograde cholangiopancreatography pancreatitis, as human acinar cells, unlike animal acinar cells, do not have functional CCK receptors [24,25].

We identified significant increases in both the serum amylase value and tissue water content at 180 min, as well as morphologically evident intestinal edema at 120 and 180 min after PDL. These biochemical and morphological findings are compatible with those made in past studies [26,27]. However, we consider that these findings (under conditions with no tissue necrosis), which were detected at 180 min after PDL, may have been due not to an increase in vascular permeability but rather one in paracellular permeability among the acini. In the present study, we made 3 important findings in our immunofluorescence and ultrastructural studies: i) there were less distinct acinar lumens, as indicated by TJ proteins (ZO-1), at 120 and 180 min after PDL than in the control and sham groups, ii) there were no changes in AJ proteins (pan-cadherin and beta-catenin) up to and including 180 min after PDL, and iii) there was an increase in non-closed, leaky TJs at 120 and 180 min after PDL in the ultrastructural study. These findings, observed in an early phase of pancreatitis after PDL, support the presence of increased paracellular permeability. Although both TJ and AJ alterations in acinar cells can occur (by decreased luminal pH from the secreted zymogen granules) in the supramaximal segretagogue stimulation model [28], the present results exhibiting TJ alteration alone might be a reflection of model differences.

We detected the unique morphology "focal acinar-cell necrosis" in a few samples at 60 min after PDL and in all at both 120 and 180 mins. We found misplaced exocytotic images in no ultrastructural specimens, indicating that this acinar change was not true necrosis. "Focal acinar-cell necrosis" might therefore be a reflection of derangements of inter-acinar cell-cell junctions due to the disruption of the normally continuous epithelial lining of acinar cells. In a canine duct-hypertension model, the disruption of the continuous epithelial lining at the junction between duct cells and acinar cells and the deposition of intercellular luminal content between acinar cells and the basal lamina have been reported [29]. Furthermore, the freeze-fracture method in a canine duct-hypertension model showed that some morphologic subtypes of TJs in acinar cells were observed only in the duct-hypertensive state [30]. Similarly, hepatocytes after the bile duct ligation procedure exhibited TJ alterations that decreased the colocalization of ZO-1 and claudins 1 and 2 and upregulated ZO-2 [31]. These findings seem parallel the present results. In obstructive jaundice, TJ alteration in the intestine was reportedly restored by bombesin and neurotensin [32]. Such neurotransmitters might also improve TJ alteration in the pancreas.

In conclusion, acinar TJ alterations occurred in an early phase in a rat PDL model. This change is considered likely to contribute to interstitial edema formation and might be expected to be seen in human biliary or post-endoscopic retrograde cholangiopancreatography pancreatitis.

Conflicts of Interest

The authors declare that they have no conflicts of interest.

References

1. Lerch MM, Saluja AK, Dawra R, et al (1992) Acute necrotizing pancreatitis in the opossum: Earliest morphological changes involve acinar cells. Gastroenterology 103: 205-213.

2. Chan YC, Leung PS (2007) Angiotensin II type 1 receptor-dependent nuclear factor –kB activation-medicated proinflammatory actions in a rat model of obstructive acute pancreatitis. J Pharmacol Exp Ther 323: 10-8.

3. Vigna SR, Shahid RA, Nathan JD, et al. (2011) Leukotriene B4 mediates inflammation via TRPV1 in duct obstruction-induced pancreatitis in rats. Pancreas 40(5): 708-714.

4. Schneider L, Hartwig W, Flemming T, et al. (2009) Protective effects and anti-inflammatory pathways of exogenous calcitonin gene-related peptide in severe necrotizing pancreatitis. Pancreatology 9(5): 662-669.

5. Lazar BA, Jancso G, Oszlacs O, et al. (2018) The insulin receptor is colocalized with the TRPV1 nociceptive ion channel and neuropeptides in pancreatic spinal and vagal primary sensory neurons. Pancreas 47(1): 110-115.

6. Li Q, Peng J (2014) Sensory nerves and pancreatitis. Gland Surg 3(4): 284-292.

7. Kloppel G, Maillet B (1993) Pathology of acute and chronic pancreatitis. Pancreas 8(6): 659-670.

8. Normann J (1998) The role of cytokines in the pathogenesis of acute pancreatitis. Am J Surg 175(1): 76-83.

9. Rau B, Paszkowski A, Lillich S, et al. (2001) Differential effects of caspase-1/interleukin-1b-converting enzyme on acinar cell necrosis and apoptosis in severe acute experimental pancreatitis. Lab Invest 81(7): 1001-1013.

10. Shimada M, Andoh A, Hata K, et al. (2002) IL-6 secretion by human pancreatic periacinar myofibroblasts in response to inflammatory mediators. J Immunol 168(2): 861-868.

11. Dumont AE, Martelli AB (1968) Pathogenesis of pancreatic edema following exocrine duct obstruction. Ann Surg 168(2): 302-329.

12. Metz J, Merlo M, Billich H, et al. (1978) Exocrine pancreas under experimental conditions. IV. Alterations of intercellular junctions between acinar cells following pancreatic duct ligation. Cell Tissue Res 186: 227-240.

13. Fallon MB, Gorelick FS, Anderson JM, et al. (1995) Effect of cerulein hyperstimulation on the paracellular barrier of rat exocrine pancreas. Gastroenterology 108(6): 1863-1872.

14. Austin JL, Peick AL, Wipfler J, et al. (1988) Effect of chronic partial pancreatic duct obstruction on pancreatic duct secretory pressure and permeability in cats. J Surg Res 44(6): 772-780.

15. Harvey MH, Wedgwood KR, Austin JA, et al. (1989) Pancreatic duct pressure, duct permeability and acute pancreatitis. Br J Surg 76(8): 859-862.

16. Tsukita S, Furuse M, Itoh M (2001) Multifunctional strands in tight junctions. Nat Rev Mol Cell Biol 2(4): 85-293.

17. Ghadially FN (1997) Cell junctions. In: Ultrastructural Pathology of the Cell and Matrix. 4th edn, Butterworth-Heinemann. Boston, USA, pp: 1171-1205.

18. Kaiser AM, Saluja AK, Sengupta A, et al. (1995) Relationship between severity, necrosis, and apoptosis in five models of experimental acute pancreatitis. Am J Physiol 269(5): C1295-C1304.

19. Samuel I, Toriumi Y, Yokoo H, et al. (1994) Ligation-induced acute pancreatitis in rats and opossums: A comparative morphologic study of the early phase. J Surg Res 57(2): 299-311.

20. Lerch MM, Saluja AK, Runzi M, et al. (1993) Pancreatic duct obstruction triggers acute necrotizing pancreatitis in the opossum. Gastroenterology 104(3): 853-861.

21. Nakamura R, Miyasaka K, Funakoshi A, et al. (1989) Interactions between bile and pancreatic juice diversions on cholecystokinin release and pancreas in conscious rats. Proc Soc Exp Biol Med 192(2):182-186.

22. Toriumi Y, Samuel I, Wilcockson DP, et al. (1993) Increased circulating cholecystokinin in obstruction-induced acute pancreatitis. II. Pancreatic duct obstruction with and without bile duct obstruction. J Surg Res 54(2): 132-135.

23. Samuel I, Toriumi Y, Wilcockson DP, et al. (1995) Bile and pancreatic juice replacement ameliorates early ligation-induced acute pancreatitis in rats. Am J Surg 169(4): 391-399.

24. Ji B, Bi Y, Simeone D, et al. (2001) Human pancreatic acinar cells lack functional responses to cholecystokinin and gastrin. Gastroenterology 121(6): 1380-1390.

25. Reubi JC, Waser B, Gugger M, et al. (2003) Distribution of CCK1 and CCK2 receptors in normal and diseased human pancreatic tissue. Gastroenterology 125(1): 98-106.

26. Walker NI (1987) Ultrastructure of the rat pancreas after experimental duct ligation. I. The role of apoptosis and intraepithelial macrophages in acinar cell deletion. Am J Pathol 126(3): 439-451.

27. Ohshio G, Saluja A, Steer ML (1991) Effects of short-term pancreatic duct obstruction in rats. Gastroenterology 100(1): 196-202.

28. Behrendorff N, Floetenmeyer M, Schwiening C, et al. (2010) Protons released during pancreatic acinar cell secretion acidify the lumne and contribute to pancreatitis in mice. Gastroenterology 139(5): 1711-1720.

29. Bockman DE, Schiller WR, Anderson MC (1971) Route of retrograde flow in the exocrine pancreas during ductal hypertension. Arch Surg 103(2): 321-329.

30. Akao S, Oya M, Akiyama H, et al. (2000) The tight junction of pancreatic exocrine cells is a morphometrically dynamic structure altered by intraductal hypertension. J Gastroenterol 35(10): 758-767.

31. Maly LP, Landmann L (2008) Bile duct ligation in the rat causes upregulation of ZO-2 and decreased colocationzation of claudins with ZO-1 and occludin. Histochem Cell Biol 129: 289-299.

32. Assimakopoulos SF, Vagianos CE, Charonis AS, et al. (2006) Esperimental obstructive jaundice alters claudin-4 expression in intestinal mucosa: Effect of bombesin and neurotensin. World J Gastroenterol 12(21): 3410-3415.

*Corresponding author: Sho Ogata, MD, Department of Pathology and Laboratory Medicine, National Defense Medical College, 3-2 Namiki, Tokorozawa, Saitama, 359-851, Japan; Tel: +81-4-2995-1505; Fax: +81-4-2996-5192; Email: sogata@ndmc.ac.jp

Citation: Ogata S, Tsuwano S, Tamai S, Nakanishi K (2018) Acinar Tight Junctions are Altered in an Early Phase of Acute Edematous Pancreatitis in a Rat Pancreatic Duct Ligation Model. *Ann Biomed Res* 1(2): 108.